

Topologically Protecting Squeezed Light on a Photonic Chip

Ruo-Jing Ren,^{1,2} Yong-Heng Lu,^{1,2} Ze-Kun Jiang,^{1,2} Jun Gao,^{1,2} Wen-Hao Zhou,^{1,2} Yao Wang,^{1,2} Zhi-Qiang Jiao,^{1,2} Xiao-Wei Wang,^{1,2} Alexander S. Solntsev,³ and Xian-Min Jin^{1,2,*}

¹*Center for Integrated Quantum Information Technologies (IQIT), School of Physics and Astronomy and State Key Laboratory of Advanced Optical Communication Systems and Networks, Shanghai Jiao Tong University, Shanghai 200240, China*

²*CAS Center for Excellence and Synergetic Innovation Center in Quantum Information and Quantum Physics, University of Science and Technology of China, Hefei, Anhui 230026, China*

³*School of Mathematical and Physical Sciences, University of Technology Sydney, Ultimo, New South Wales 2007, Australia*
(Dated: February 5, 2022)

Squeezed light is a critical resource in quantum sensing and information processing. Due to the inherently weak optical nonlinearity and limited interaction volume, considerable pump power is typically needed to obtain efficient interactions to generate squeezed light in bulk crystals. Integrated photonics offers an elegant way to increase the nonlinearity by confining light strictly inside the waveguide. For the construction of large-scale quantum systems performing many-photon operations, it is essential to integrate various functional modules on a chip. However, fabrication imperfections and transmission crosstalk may add unwanted diffraction and coupling to other photonic elements, reducing the quality of squeezing. Here, by introducing the topological phase, we experimentally demonstrate the topologically protected nonlinear process of spontaneous four-wave mixing enabling the generation of squeezed light on a silica chip. We measure the cross-correlations at different evolution distances for various topological sites and verify the non-classical features with high fidelity. The squeezing parameters are measured to certify the protection of cavity-free, strongly squeezed states. The demonstration of topological protection for squeezed light on a chip brings new opportunities for quantum integrated photonics, opening novel approaches for the design of advanced multi-photon circuits.

Over the last few decades, researchers have witnessed the emerging field of quantum information[1]. Various advances have been achieved in a plethora of hardware platforms[2, 3]. Photon, due to its fast spread and robustness against the thermal environment, is considered as a perfect information carrier for quantum information processing[4, 5]. Thus, quantum light sources, particularly indistinguishable correlated photon pairs, are kernel resource for quantum communication[6, 7] and quantum computation[8–11]. Besides these researches focusing on Fock-like states, squeezed light also serves as another fundamental resources for quantum information[12–15]. Spontaneous parametric frequency conversion in nonlinear crystals is an indispensable approach in quantum optics to obtain the non-classical light[16, 17], as well as to generate multi-photon entangled states[18–21].

In order to obtain a strong nonlinear interaction in a bulk crystal, a tight focusing condition is required, however, which would lead to a small Rayleigh length limiting the interaction volume. The pump light power consumption in the bulk crystals is always too large for scalability, and the pump power usually exceeds the threshold of the material, causing modulations to the micro-nano structure leading to undesired nonlinear effects. In the last few years, integrated photonics stands out by offering a compact solution[22, 23], which greatly reduces such undesirable effects by confining the pump light inside the waveguide, thus both of the tight focusing condition and interaction zone are guaranteed at the same time. The progresses in this field have been demonstrated by developing waveguide-based quantum sources by femtosecond laser writing[24], UV-laser writing[25], and silicon photonics platforms[26, 27], showing the availability and the high performances like brightness, purity and low propagation loss in a single chip. Most recent work has shown the potential of

integrated source to encode information in both discrete and continuous variables[28].

To construct large-scale photonic quantum systems, high-quality building blocks should be integrated in a compact footprint with an immense complexity[29]. Compared to the silicon photonics platform, femtosecond laser writing chips show the capability of fully 3D integration, which is particularly suitable for simulating 2D structures[30, 31], and have been used to carry out various quantum tasks[32, 33]. Supposing an on-chip source module is embedded into a complex arrangement, due to the coupling effect, crosstalk is prone to occur between adjacent waveguides. Furthermore, the intensity to maintain strong squeezing will be greatly reduced during the evolution, since the pump light would diverge into the neighboring sites. These unwanted losses break the strong confinement and cause insufficient light-matter interaction to work as a quantum squeezer. The quantum features, for example, the cross correlation and the squeezing quality of the generated photon pairs will decay as time evolves. The key challenge is to protect the nonlinearity, the related interaction process and the quantumness of the generated photon pairs simultaneously.

The topological phase allows the protection of physical fields against unavoidable disorder leading to recent demonstrations of topological protection of various nonlinear optical processes[34, 35], including photon-pair generation[36–41]. The above, however, was only studied in the regime of low photon numbers, while strongly squeezed light remained out of scope despite the significant importance of squeezing in quantum optics. In this letter, we experimentally exhibit the topological protection of the squeezed light with dimerized-type chain resembling Su-Schrieffer-Heeger (SSH) lattices on a photonic chip. We observe robust localization phenomenon

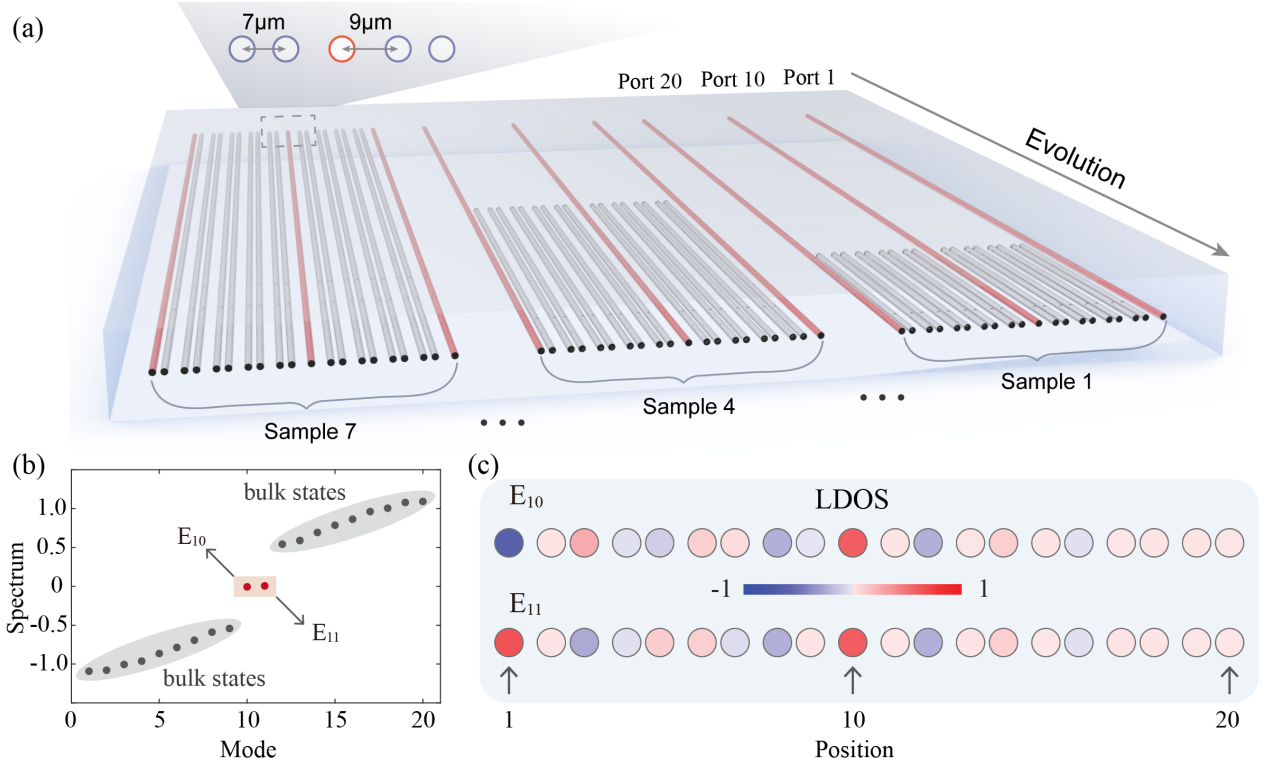


FIG. 1. **Schematic diagram of lattice with topological protection for squeezed light.** (a) The structure of the lattice with topological protection for squeezed light contain seven groups with evolution distances ranging from 5 mm to 35 mm. The short and long separation between adjacent waveguides is 7 μm and 9 μm respectively. (b) The spectrum of the lattice with topological protection for squeezed light. There are only two zero-energy modes E_{10} and E_{11} and two extended bulk bands. Modes E_{10} and E_{11} locate inside the band gap and decouple from the bulk bands, which promises the topologically protected fashion. (c) The eigenmode local density of states (LDOS) of the gapped mode E_{10} (upper line) and E_{11} (lower line) with spatial distribution. The edge states and interface-defect states are mainly localized at the 1st site and the 10th site of lattice both with high amplitude.

of the topological states at different wavelengths. We verify the topological protection of quantum resources by measuring the transport dynamics such as light filed distributions, the cross-correlations by switching incident pump light into different input ports. The squeezing parameters are particularly measured under different evolution distances. Our results demonstrate that the topological protection is robust to different wavelengths of non-classical states, and can help to construct quantum squeezers in an engineered structure against imperfections.

Our topologically protected lattices are inscribed on a 20 mm \times 35 mm \times 1 mm fused silica substrate by femtosecond laser direct writing. The writing laser has a wavelength of 513 nm, and a repetition rate of 1 MHz. Based on our previous work[28], the waveguide itself can function as a Spontaneous Four Wave Mixing (SFWM) source, following energy and momentum conservation, $2\hbar\omega_p = \hbar\omega_s + \hbar\omega_i$ and $2\hbar k_p = \hbar k_s + \hbar k_i$, where k indicates the momenta of the field. The material absorbs two photons from the pump wave, and generates signal and idler photon pairs, where the birefringence induced phase matching condition is fulfilled by

$$\Delta k = \frac{2[n(\omega_p) + \Delta n]\omega_p}{c} - \frac{n(\omega_s)\omega_s}{c} - \frac{n(\omega_i)\omega_i}{c} = 0. \quad (1)$$

Here the birefringence Δn dominates the phase matching condition.

The constructed topologically protected quantum light lattices, being composed of small and large spacing with adjacent waveguides, corresponding to the modulation of alternating weak (J_1) and strong (J_2) couplings, which can be described by the following Hamiltonian,

$$H = \sum_n (J_1 a_n^\dagger b_n + J_2 b_n^\dagger a_{n+1}) + h.c. \quad (2)$$

The lattices possess two topologically protected channel: the edge-state channel and the interface-defect channel, as shown in Fig.1(a). Here, we set the separation distances $l_1=7 \mu\text{m}$ and $l_2=9 \mu\text{m}$ respectively. The dimerized-type chain resembling SSH model[42] possesses and enables topological non-trivial phases with edge states described by the bulk-edge correspondence[43, 44]. The edge states can be regarded as the topological transition interface between trivial vacuum and nontrivial lattice structure. In addition, the interface-defect channel in the middle of the lattice acts as a topologically protected interface states[45] by interfacing two versions of the dimerization patterns with distinct Zak phases[46, 47], which is supported by the existence of the topological phase transi-

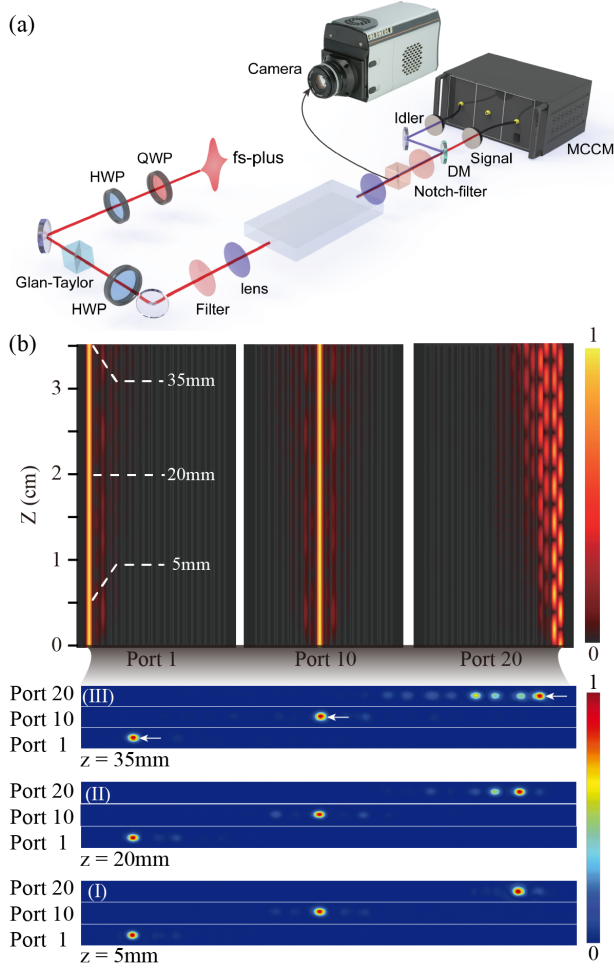


FIG. 2. Experimental setup and intensity distributions of the pump light. (a) Experimental setup for generation, filtering and evolution measurement of the quantum light source. The input ports can be easily switched among different groups. DM: dichroic mirror, MCCM: multi-channel coincidence module. (b) Simulated intensity distributions of the pump light from port 1, 10 and port 20. The evolution distance is marked in white color. (I)(II)(III) show the experimentally measured intensity distributions from three input channel ports at 5 mm, 20 mm and 35 mm evolution distances respectively. The protected states from port 1 and 10 always maintain localization as the traveling distance increases while the unprotected state from port 20 diffuses over the lattice. The intensity distribution is normalized to its maximum.

tion between them.

We further illustrate the band diagram by characterizing the spectrum of the lattice, as shown in the Fig.1(b). The band diagram contains two extended bands separated by the band gap. Inside the band gap, there are two modes E_{10} and E_{11} pinning on the quasi zero energy level with decoupling from the bulk band, which reveals the existence of the topological gapped edge states. The spatial distribution can be characterized by the eigenmode local density of states (LDOS)[48], which can be defined by $D_n(E) = \sum_m \delta(E - E_m) \psi_n^m$, where E is the energy of the m^{th} eigenstate $\psi(m)$ and n is the site label. As

shown in Fig.1(c), the LDOS of the two gapped modes indicates that the modal amplitude with maxima appears in sites 1^{st} and 10^{th} site, while the minima appears in other sites in both two modes. This shows the localization in the edge channel and interface-defect channel under the norm of the topologically protected zero-energy modes. In contrast, the low amplitude occupying at 20^{th} site shows that the edge channel in 20^{th} port is trivial with dominated bulk modes rendering photons diffuse into bulk of the lattice. Therefore, among the three input ports in the lattice with topological protection for squeezed light (depicted in Fig.1(b)), the edge-state channel port 1 and the interface-defect channel port 10 both are topologically protected, and the edge channel port 20 is the trivial one.

The experimental setup is schematically depicted in Fig.2(a), the mode-locked 780 nm femtosecond pump pulses (80 MHz) of vertical polarization (prepared by a combination of waveplates and Glan-Taylor polarizer) are injected and switched into three different channel ports, namely 1, 10 and 20. The output light intensity distributions of the pump light are accumulated by a CCD camera, and the evolution patterns under different distances varying from 5 mm to 35 mm (see I, II, and III in Fig.2(b)) are also recorded. We experimentally verify the localization effect in the above 3 ports by comparing the measured pattern with theoretical simulation results in Fig.2(b). It is obvious that the pump light propagates locally as time evolves in the edge-state channel and the interface-defect channel (the topological ones), while the beam diffuses and gradually couples to the adjacent sites in the edge channel port 20 (the trivial one). The localization effect of the above topological channel ports indicates valid protection of the pump intensity, and provides sufficient power for generating quantum source during nonlinear interaction process. The diffusion degrades the intensity as the propagation length increases, and the decreased pump intensity fails to achieve a high quality quantum source during the SFWM process. It can be deduced that the nonlinearity processes in port 1 and port 10 are well protected at the wavelength of 780 nm. The pump light is spatially protected and the good localization effect makes the subsequent nonlinear process more efficient.

After verifying the spatial protection effect of the pump light, we further test whether the on-chip generated correlated photons can still be well protected. We first calculate the light intensity distributions of the signal and idler photons, and the theoretical simulation results are presented in Fig.3(a) and (b) respectively. Even for light with different wavelengths, the localization effect still emerges in the topologically protected channels. To retrieve the signal and idler photons, we first filter out the residual pump light using both the polarization filter (Glan-Taylor polarizer) and the spectrum filter (notch filters centered as 780 nm). Then, the signal and idler photons are separated into two different spatial modes by a dichroic mirror, where the idler photons transmit while the signal photons are reflected. The photon pairs are coupled into single mode fibers, and then detected by avalanche photodiodes. All the coincidence counts are recorded by a homemade multi-

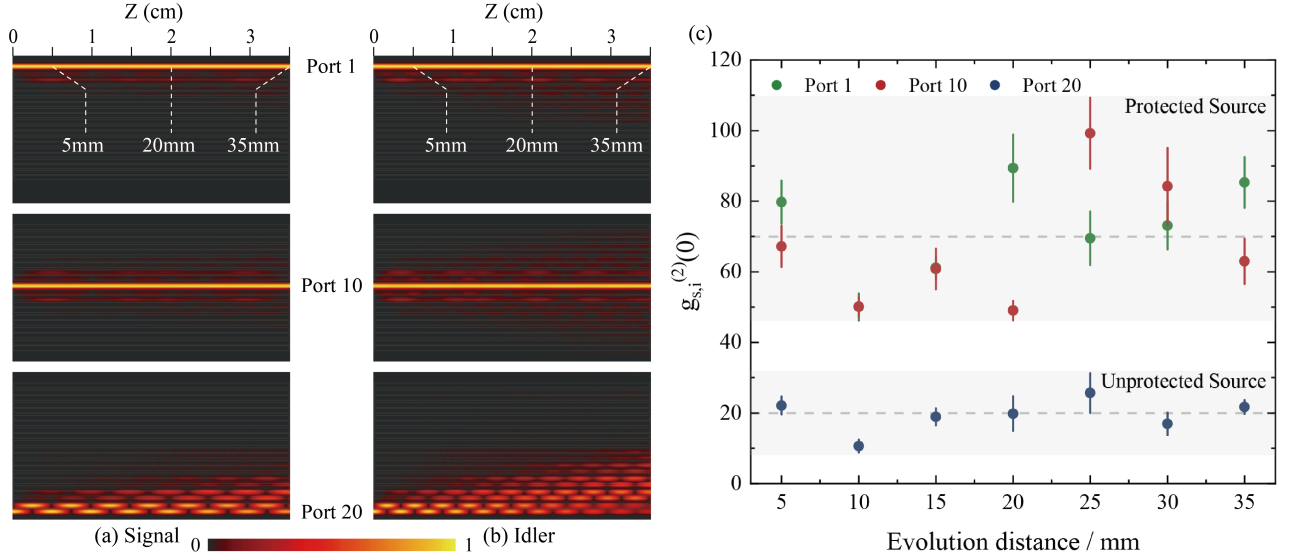


FIG. 3. **Performance of topological protection for the generated photon pairs.** (a) The evolution result of the signal photon from different input ports. (b) The evolution result of the idler photon from different input ports. (c) The cross correlation $g_{si}^{(2)}(0)$ of different channel entrances 1, 10 and 20 evolving from 5 mm to 35 mm with a step of 5 mm are measured. The cross correlation $g_{si}^{(2)}(0)$ of channel port 1 and 10 are depicted in green and red colors respectively with high values, which demonstrate the protection of the nonlinear process in the topological structures. The cross correlation $g_{si}^{(2)}(0)$ of channel port 20 is depicted in blue color, and the values are about five times lower than the protected states from channel port 1 and 10.

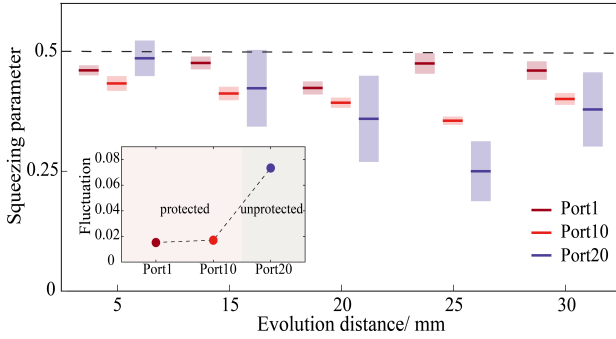


FIG. 4. **Experimental verification of topological protection for the squeezing parameters.** The squeezing parameters of the channel port 1, 10 and 20 are depicted in deep red, red and blue colors accordingly. The values of the squeezing parameters are more uniform and higher in two protected channel input ports compared with the unprotected channel port 20. The variance between three topological channels are obviously different since the unprotected channel port 20 fluctuates in a larger range. The inset shows the average fluctuation from each import. Compared to the results of the other two channel ports, the channel port 20 is unprotected.

channel coincidence module. The experiment layout can be found in Fig.2(a). To quantify the non-classical feature of the correlated photon pairs, we introduce the cross-correlation function as follows,

$$g_{s-i}^{(2)}(0) = \frac{\langle \hat{a}_s^\dagger \hat{a}_i^\dagger \hat{a}_i \hat{a}_s \rangle}{\langle \hat{a}_s^\dagger \hat{a}_s \rangle \langle \hat{a}_i^\dagger \hat{a}_i \rangle} \quad (3)$$

A value higher than 2 of the cross-correlation function $g_{s-i}^{(2)}(0)$ is a strong evidence of quantum feature, for instance, the violation of Bell inequality requires $g_{s-i}^{(2)}(0)$ larger than 6[49].

The cross correlation $g_{s-i}^{(2)}(0)$ of the edge-state channel port 1 vary from 50.03 ± 3.85 to 89.34 ± 9.53 with evolution distances from 5 mm to 35 mm, which is a strong evidence of non-classical correlation. The cross correlation $g_{s-i}^{(2)}(0)$ of the interface-defect channel port 10 vary from 49.01 ± 2.75 to 99.25 ± 10.07 , indicating the protection of SFWM photon pair generation process. Under the same transport length, in contrast, the cross correlation $g_{s-i}^{(2)}(0)$ of the unprotected edge channel port 20 only vary from 10.58 ± 1.82 to 25.65 ± 5.6 . As can be seen from the Fig.3(c), the topologically protected structure can provide nearly five times higher cross correlation than that in the unprotected states. If the evolution length continues to increase, the loss and decoherence will become more serious, and these eventually turn into the critical obstacles against protecting the nonlinear photon generation process.

Due to the strong confinement of the pump light, our source can function as squeezed light source[50] in the high power regime. The threshold of fused silica is very robust, thus, combined with the engineered topological structures, both weak pump and strong pump regimes can be protected. In the weak pump regime, the discrete variables such as heralded photon sources are protected, while in the strong pump regime, the high-order terms of the nonlinear process and the squeezing parameters are dominant. We further explore the squeezing parameters among three different topological structures. The squeezing parameter λ can be calculated by measuring the

auto-correlation function $g_H^{(2)}(0)$ and the heralding efficiency η_H using the following formula,

$$\lambda^2 = g_H^{(2)}(0) \frac{\eta_H}{2(1 - (1 - \eta_H)^2)}. \quad (4)$$

As shown in Fig.4, the squeezing parameters of the three channel ports are depicted in different colors under different evolution distances, where two distinct features can be observed. In the long evolution distance regimes, the squeezing parameters of the topologically protected channels are larger than the unprotected channels. In addition, the measured fluctuations using Poissonian statistics in port 20 are greatly influenced by the beam diffusion. These results indicate that the squeezed states can be well protected in the topological structure.

In conclusion, we have reported the topological protection of on-chip SFWM and the generated squeezed light. By introducing a topological phase with a dimerized-type chain resembling SSH lattices on a silica photonic chip, we have observed the localization and strong confinement of the pump light in the topologically protected channels. The protected pump light field fulfils the tight focusing condition to allow the waveguide to function as a high-quality quantum squeezer. We have demonstrated that the protection applies to different wavelengths, impacting the cross-correlations and the squeezing parameters. It showcases a robust generation of quantum resources for future practical quantum information tasks, such as Gaussian boson sampling applications and bosonic error correction codes. We have verified the validity of the topological protection of on-chip squeezers, which may play an essential role in photonic quantum information processing[51].

The authors thank Jian-Wei Pan for helpful discussions. This research is supported by National Key R&D Program of China (2019YFA0308700, 2019YFA0706302 and 2017YFA0303700), National Natural Science Foundation of China (NSFC) (11904229, 61734005, 11761141014, 11690033), Science and Technology Commission of Shanghai Municipality (STCSM) (20JC1416300, 2019SHZDZX01), Shanghai Municipal Education Commission (SMEC)(2017-01-07-00-02-E00049). X.-M.J. acknowledges additional support from a Shanghai talent program. X.-M.J. acknowledges support from the National Young 1000 Talents Plan and support from Zhiyuan Innovative Research Center of Shanghai Jiao Tong University. A. S. S. Acknowledges support from Australian Research Council (DE180100070) and University of Technology Sydney Seed Fund.

* xianmin.jin@sytu.edu.cn

[1] M. Nielsen and I. Chuang, Quantum Computation and Quantum Information. Cambridge University Press (2000).

- [2] T. D. Ladd, *et al.* Quantum Computers. *Nature* **464**, 45 (2010).
- [3] G. Popkin, Quest for Qubits. *Science* **354**, 1090 (2016).
- [4] L. Mandel and E. Wolf, Optical Coherence and Quantum Optics. Cambridge University Press (1995).
- [5] J. L. O'Brien, A. Furusawa and J. Vučković, Photonic quantum technologies. *Nature Photon.* **3**, 687 (2009).
- [6] N. Gisin, G. Ribordy, W. Tittel and H. Zbinden, Quantum Cryptography. *Rev. Mod. Phys.* **74**, 145 (2002).
- [7] F. Xu, X. Ma, Q. Zhang, H.-K. Lo and J.-W. Pan, Secure Quantum Key Distribution with Realistic Devices. *Rev. Mod. Phys.* **92**, 025002 (2020).
- [8] C. K. Hong, Z. Y. Ou and L. Mandel, Measurement of Subpicosecond Time Intervals between Two Photons by Interference. *Phys. Rev. Lett.* **59**, 2044 (1987).
- [9] P. Kok, *et al.* Linear Optical Quantum Computing with Photonic Qubits. *Rev. Mod. Phys.* **79**, 135 (2007).
- [10] M. Lebugle, *et al.* Experimental Observation of N00N State Bloch Oscillations. *Nat. Commun.* **6**, 8273 (2015).
- [11] C. Sparrow, *et al.* Simulating the Vibrational Quantum Dynamics of Molecules Using Photonics. *Nature* **557**, 660 (2018).
- [12] S. L. Braunstein and P. van Loock, Quantum Information with Continuous Variables, *Rev. Mod. Phys.* **77**, 513 (2005).
- [13] C. Weedbrook, *et al.* Gaussian Quantum Information, *Rev. Mod. Phys.* **84**, 621 (2012).
- [14] C. S. Hamilton, *et al.* Gaussian Boson Sampling, *Phys. Rev. Lett.* **119**, 170501 (2017).
- [15] D. Gottesman, A. Kitaev and J. Preskill, Encoding a Qubit in an Oscillator. *Phys. Rev. A* **64**, 012310 (2001).
- [16] C. Kurtsiefer, M. Oberparleiter and H. Weinfurter, Generation of Correlated Photon Pairs in Type-II Parametric Down Conversion—Revisited. *J. Mod. Opt.* **48**, 1997 (2001).
- [17] L. Caspani, *et al.* Integrated Sources of Photon Quantum States Based on Nonlinear Optics. *Light Sci. Appl.* **6**, e17100 (2017).
- [18] P. G. Kwiat, *et al.* New High-Intensity Source of Polarization-Entangled Photon Pairs. *Phys. Rev. Lett.* **75**, 4337 (1995).
- [19] J.-W. Pan, M. Daniell, S. Gasparoni, G. Weihs and A. Zeilinger, Experimental Demonstration of Four-Photon Entanglement and High-Fidelity Teleportation. *Phys. Rev. Lett.* **86**, 4435 (2001).
- [20] X.-L. Wang, *et al.* Experimental Ten-Photon Entanglement. *Phys. Rev. Lett.* **117**, 210502 (2016).
- [21] H.-S. Zhong, *et al.* 12-Photon Entanglement and Scalable Scattershot Boson Sampling with Optimal Entangled-Photon Pairs from Parametric Down-Conversion. *Phys. Rev. Lett.* **121**, 250505 (2018).
- [22] J.-W. Wang, F. Sciarrino, A. Laing and M. G. Thompson, Integrated Photonic Quantum Technologies. *Nat. Photonics* **14**, 273 (2020).
- [23] F. Flamini, N. Spagnolo and F. Sciarrino, Photonic Quantum Information Processing: a Review. *Rep. Prog. Phys.* **82**, 016001 (2019).
- [24] J. B. Spring, *et al.* On-chip Low Loss Heralded Source of Pure Single Photons. *Opt. Express* **21**, 13522 (2013).
- [25] J. B. Spring, *et al.* A Chip-based Array of Near-identical, Pure, Heralded Single Photon Sources. *Optica* **4**, 90 (2017).
- [26] J. W. Silverstone, *et al.* On-chip Quantum Interference between Silicon Photon-pair Sources. *Nature Photon.* **8**, 104 (2014).
- [27] S. Paesani, *et al.* Near-ideal Spontaneous Photon Sources in Silicon Quantum Photonics. *Nat. Commun.* **11**, 2505 (2020).
- [28] R.-J. Ren, *et al.* 128 Identical Quantum Sources Integrated on a Single Silica Chip. arXiv preprint arXiv:2005.12918
- [29] J.-W. Wang, *et al.* Multidimensional Quantum Entanglement with Large-scale Integrated Optics. *Science* **360**, 285 (2018).
- [30] K. M. Davis, K. Miura, N. Sugimoto and K. Hirao, Writing Waveguides in Glass with a Femtosecond Laser. *Opt. Lett.* **21**,

- 1729 (1996).
- [31] R. Osellame, G. Cerullo and R. Ramponi, Femtosecond Laser Micromachining: Photonic and Microfluidic Devices in Transparent Materials, Topics in Applied Physics. (Springer, 2012).
 - [32] H. Tang, *et al.* Experimental Two-dimensional Quantum Walk on a Photonic Chip. *Sci. Adv.* **4**, 3174 (2018).
 - [33] H. Tang, *et al.* Experimental Quantum Fast Hitting on Hexagonal Graphs. *Nature Photon.* **12**, 754 (2018).
 - [34] D. Leykam, A. S. Solntsev, A. A. Sukhorukov and A. S. Desyatnikov, Lattice Topology and Spontaneous Parametric Down-conversion in Quadratic Nonlinear Waveguide Arrays. *Phys. Rev. A* **92**, 033815 (2015).
 - [35] D. Smirnova, D. Leykam, Y. Chong and Y. Kivshar, Nonlinear Topological Photonics. *Appl. Phys. Rev.* **7**, 021306 (2020).
 - [36] A. Blanco-Redondo, *et al.* Topological Protection of Biphoton States. *Science* **362**, 568 (2018).
 - [37] M. Wang, *et al.* Topologically Protected Entangled Photonic States. *Nanophotonics* **8**, 1327 (2019).
 - [38] K. Tschernig, *et al.* Topological Protection Versus Degree of Entanglement of Two-photon Light in Photonic Topological Insulators. *Nat. Commun.* **12**, 1974 (2021).
 - [39] M. C. Rechtsman, *et al.* Topological Protection of Photonic Path Entanglement. *Optica* **3**, 925 (2016).
 - [40] Y. Wang, *et al.* Topological Protection of Two-photon Quantum Correlation on a Photonic Chip. *Optica* **6**, 955 (2019).
 - [41] Y. Wang, *et al.* Topologically Protected Quantum Entanglement. arXiv preprint arXiv:1903.03015
 - [42] W. P. Su, J. R. Schrieffer and A. J. Heeger, Solitons in Polyacetylene. *Phys. Rev. Lett.* **42**, 1698 (1979).
 - [43] L. Lu, J. D. Joannopoulos and M. Soljacic, Topological Photonics. *Nature Photon.* **8**, 821 (2014).
 - [44] T. Ozawa, *et al.* Topological Photonics. *Rev. Mod. Phys.* **555**, 015006 (2019).
 - [45] A. Blanco-Redondo, *et al.* Topological Optical Waveguiding in Silicon and the Transition between Topological and Trivial Defect States. *Phys. Rev. Lett.* **116**, 163901 (2016).
 - [46] J. Zak, Berry's Phase for Energy Bands in Solids. *Phys. Rev. Lett.* **62**, 2747 (1989).
 - [47] P. Delplace, D. Ullmo and G. Montambaux, Zak Phase and the Existence of Edge States in Graphene. *Phys. Rev. B* **84**, 195452 (2011).
 - [48] J. Noh, *et al.* Topological Protection of Photonic Mid-gap Defect Modes. *Nature Photon.* **12**, 408 (2018).
 - [49] H. de Riedmatten, *et al.* Direct measurement of decoherence for entanglement between a photon and stored atomic excitation. *Phys. Rev. Lett.* **97**, 113603 (2006).
 - [50] A. I. Lvovsky, Squeezed Light, arXiv preprint arXiv:1401.4118
 - [51] J. M. Arrazola, *et al.* Quantum Circuits with Many Photons on a Programmable Nanophotonic Chip. *Nature* **591**, 54 (2021).